Energy production and sanitation improvement using microbial fuel cells

I. Ieropoulos, J. Greenman, D. Lewis and O. Knoop

ABSTRACT

This study builds on the previous work of urine utilisation and uses small-scale microbial fuel cells (MFCs), working both as individual units in cascade or collectively as a stack, to utilise artificial urine. Artificial urine was prepared at concentrations typically found in real human urine with peptone employed as a surrogate proteinacious component. MFCs were constructed from Nanocure® polymer using rapid prototype technology. The anode and cathode electrodes were made of 15 cm^2 carbon veil, folded down to fit in the 1 mL chambers. Eight MFCs were inoculated using activated anaerobic sludge; after 17 days of fed batch mode they were switched to continuous flow, initially at 0.09 mL/h and subsequently at 0.43 mL/h, resulting in HRT of 12.69 minutes/MFC. MFCs showed stable performance following the maturing period and produced, under polarisation experiments, peak power levels of 117 μW, corresponding to 962.94 W/m^3. Continuous flow experiments data showed higher power production, increasing with the concentration of the carbon/energy source within artificial urine. The work demonstrates that artificial urine of varying composition can be successfully utilised for the production of energy and concomitant cleanup of organic waste. Finally, in line with the practical implementation and robotics work in our group, the small-scale MFCs were configured into a stack and directly energised electronic devices.

Key words | microbial fuel cells, practical application, sanitation, urine, waste utilisation

I. Ieropoulos (corresponding author)
D. Lewis
Bristol Robotics Laboratory,
University of the West of England and University of Bristol,
T-Building,
Frenchay Campus,
Coldharbour Lane,
BS16 1QY,
UK
E-mail: *ioannis.ieropoulos@brl.ac.uk*

J. Greenman
Centre for Research in Biosciences,
University of the West of England,
Bristol,
UK

O. Knoop
Universität Duisburg-Essen,
Germany

INTRODUCTION

Microbial fuel cells (MFCs) are unique bio-electrochemical transducers that convert wet organic waste directly into electricity, through the metabolism (waste treatment) of constituent microorganisms. One such global and abundant waste product is human or animal urine, which has already been demonstrated to be an efficient fuel for direct electricity production via single MFCs with >50% efficiency (Ieropoulos *et al*. 2012). The MFC is a true green technology that operates within the immediate carbon cycle and does not rely on fossil fuels, but it also carries the added advantage of low cost manufacture and maintenance. MFCs are therefore a potential sustainable energy source for the future that concomitantly produces clean water and cleaner effluent, advantageous for developed and developing countries (Ieropoulos *et al*. 2012). The latter would directly impact the wastewater treatment challenge, by relieving existing treatment systems from heavy organic and inorganic loading, thereby improving sanitation.

Improved energy outputs and scale-up of the technology are most likely to be achieved through miniaturisation and multiplication of MFC units and thus careful fine tuning of the key parameters governing the performance of stacks of miniaturised MFCs is critical (Ieropoulos *et al.* 2008, 2010a; Fangzhou *et al.* 2011; Qian & Morse 2011). Some of the parameters that have already been considered include the inoculum source and community mix (Ieropoulos *et al.* 2010a; Zhang *et al.* 2012); substrate (Futamata *et al.* 2012; Yu *et al.* 2012); catholyte (Harnisch & Schröder 2010; Zhang *et al.* 2012); MFC structural material (Ieropoulos *et al.* 2010a); flow rate (Ieropoulos *et al.* 2010c; Ledezma *et al.* 2012; Winfield *et al.* 2012); anode material (He et al. 2012; Liu *et al.* 2012); anode chamber volume to electrode surface

doi: 10.2166/washdev.2013.117

area (Ieropoulos 2006) and the type of proton exchange membrane (Ieropoulos *et al.* 2010a).

The overall aim of our work was to investigate the performance of novel small-scale MFCs (2 mL volume) assembled in a stack configuration, fed with artificial urine and demonstrate their practical implementation by directly powering electronic devices. The stack was configured in a cascade manner, where all MFC units were hydraulically linked, in an attempt to sequentially treat the urine fuel at different added carbon-energy concentrations and thus better utilise the organic contents. Several other key parameters were investigated for improving the energy output and two electronic devices were powered; LEDs and a dc motor driving a toy windmill.

MATERIALS AND METHODS

Inoculum source and set-up

Anaerobic activated sewage sludge was provided by Wessex Water (Saltford, UK). Samples were initially kept in their original water-based suspension at 4 °C and stored for three months. Prior to the experiments, sludge samples were mixed with 1% peptone, 0.5% yeast extract (Oxoid, Basingstoke, UK) and allowed to acclimatise at room temperature before inoculating the whole connected stack (eight MFCs) with 20 mL of sludge, downstream through MFC1, and kept in batch mode for 17 days (Figure 1).

The initial inoculum was replaced on days 3, 6, 7, 8, 9, 10, 13 and 14 in the same manner. On day 18, the stack was fed with artificial urine medium (AUM) as described by Brooks & Keevil (1997) with the exception of tetrasodium pyrophosphate added at a concentration of 0.006 g/L to prevent precipitation (Sigma-Aldrich, Dorset, UK). AUM was then filter sterilised with a 0.2 μm filter (Merck Millipore, Ireland). AUM was fed initially on a continuous flow rate of 0.086 mL/h to the MFC stack using a peristaltic pump (Waston Marlow 101 U/R). On day 21 (from the initial inoculation) this was increased to 0.43 mL/h. On day 23, the carbon energy (i.e. peptone and yeast extract) concentration in AUM was increased to 15× (AUM 15×) to

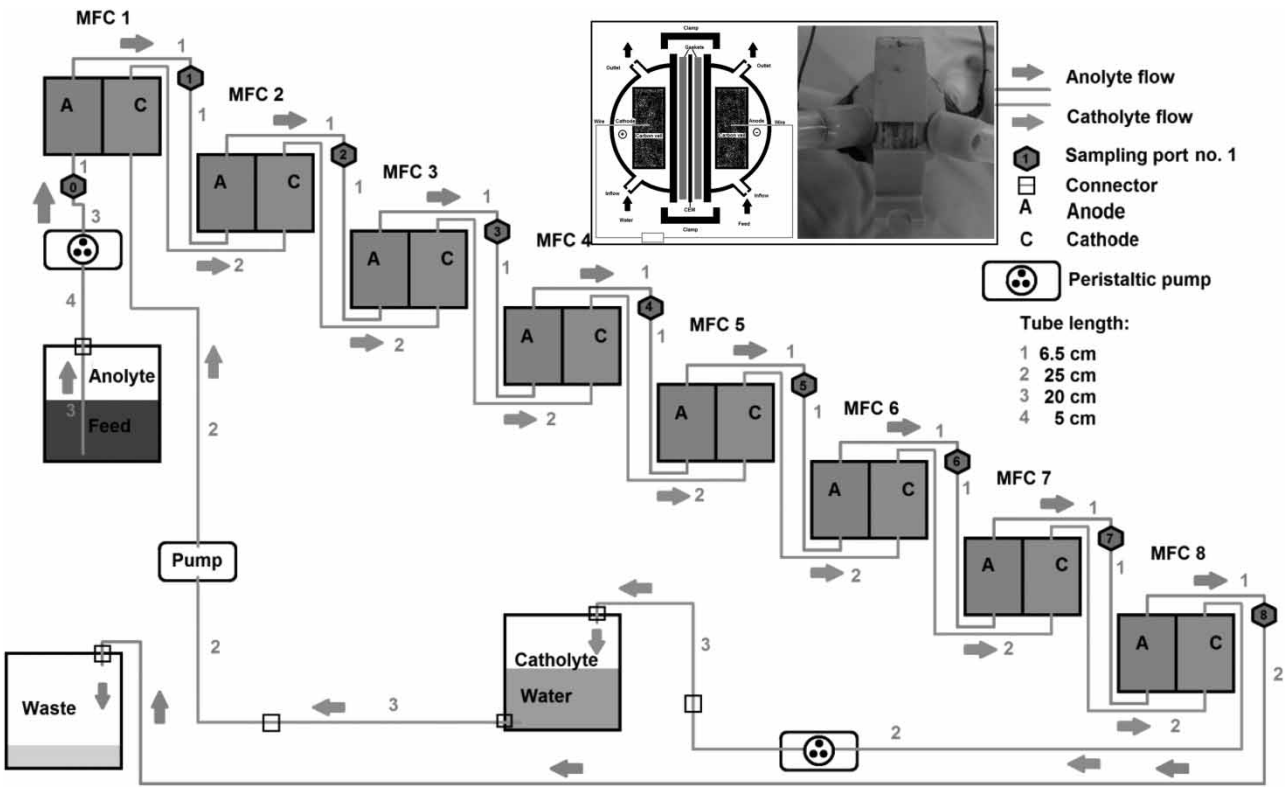

Figure 1 | Set-up of eight MFCs as a cascade. Inset: (Left) Schematic diagram of the small-scale MFC and (right) Photograph of an actual small-scale MFC. Total height is 2.54 cm.

accelerate the growth of the anodophilic microorganisms. Carbon energy (C/E) concentrations of AUM 2× and AUM 5× were also vestigated as part of the carbon energy concentration experiments.

Tap water was used as the catholyte, recirculated by a different peristaltic pump (Welco WPX 1, Japan) and controlled with a DC regulated power supply (DPS-1850, Manson, UK) at a flow rate of 298.27 mL/h, and was consistently refreshed every 7 days.

Small-scale MFC design

The eight small-scale MFCs were designed using the SolidEdge® CAD software and fabricated using rapid-prototype 3D-printing (Perfactory®). The structural material used was RC 25 (Nanocure®) resin, doped with ceramic nanoparticles. Anode and cathode chambers were designed to have a total volume of 1 mL, and were separated by a cation-exchange membrane (CEM) for proton transfer (CMI-7000S, Membranes International Inc, USA). Carbon veil electrodes of 15 cm^2 (30 g/m^2; PRF Composite Materials, UK) were inserted in each half-cell. Gaskets (O-rings) were used on either side of the membrane for water tightness, and were produced from two elastic compounds in equal amounts that were allowed to air-dry and cure into 2 mm thick films (Plasti Gel 00, A & B, Mouldlife Materia Innovation, UK). Figure 1 inset, shows a schematic and side-view photo of the small-scale MFC.

Conductivity of the different media

The different concentrations of AUM were diluted at a ratio of 1 : 8 in distilled water and the conductivity of these was measured by a portable multi-parameter instrument (HI991300 with a HI 1288 electrode, HANNA Instruments LTD, UK). The same apparatus was used for determining the conductivity of the tap water catholyte.

Data capture and calculations of power output

Electrode output was recorded in volts (V) against time using an ADC-16 Channel Data Logger (Pico Technology Ltd, Cambridgeshire, UK). Power output was calculated as described by Ieropoulos *et al.* (2010a).

Polarisation experiments

Polarisation experiments were performed using a load-controlled measurement tool as described by (Degrenne *et al.* 2012). The resistor range (38.4–3.74 Ω) was controlled with the Bio-Electrical Energy Management Software (v1.0.6, Laboratoire AMPERE, Ecole Centrale de Lyon, UMR CNRS 5005). The time step for each resistor load connected to the MFCs was 3 minutes; data were recorded every 30 seconds. Polarisation experiments were performed for the different AUM C/E concentrations (2×, 5× and 15×). The flow rate was kept constant at 0.450 mL/h throughout. Prior to polarisation experiments, all MFCs were left open circuit (V_{OC}) for up to 1 h, to obtain steady state values.

Electrical stack configurations

Four different electrical configurations were tested for the stack of eight MFCs, namely series, parallel and two variants of series-parallel combinations; four groups of two-in-parallel MFCs, connected in series (termed '4(2)-series') and two groups of four-in-parallel MFCs connected again in series (termed '2(4)-series'). This was in order to derive the best performing configuration for powering the electronic devices.

Practical implementation

A windmill model (SOL-EXPERT group, Ravernsberg, Germany) was used as an exemplar of a dc motor-driven device, with the MFC stack connected via a 5 Farads capacitor (DCNQ; Illinois Capacitors Inc, USA). The capacitors were used to accumulate the energy from the MFCs in order to match the power requirements of the motor, similar to the EcoBots (Ieropoulos *et al.* 2010b).

RESULTS AND DISCUSSION

Characterisation of small-scale MFCs within a cascade with increasing C/E source

Figure 2(a)–(d) shows the polarisation and power curves for MFCs 1, 4, 5 and 8, respectively, performed over a 1-week

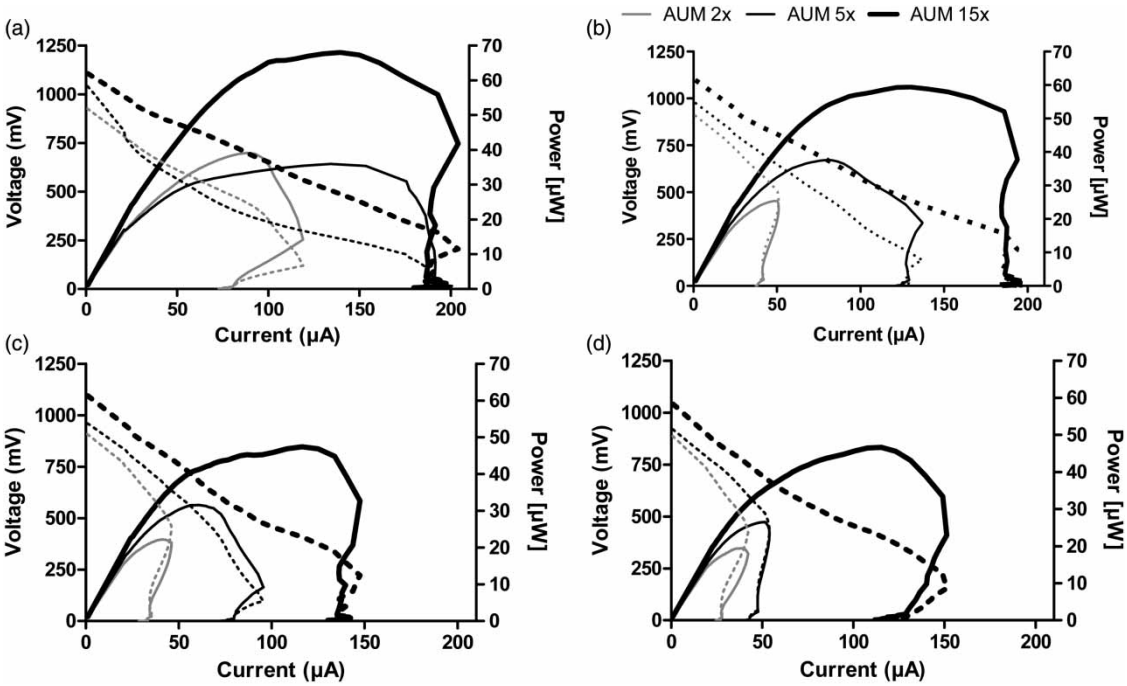

Figure 2 | Polarisation (left *y*-axis/dashed lines) and power (right *y*-axis/solid lines) curves for MFC 1 (a), MFC 4 (b), MFC 5 (c) and MFC 8 (d).

period with increasing concentrations of C/E added to the AUM. Each polarisation sweep was performed 2 days after a change of substrate. With AUM 15× as the anolyte, MFC1 produced the highest power of 67 μW with decreasing values in order of the downstream MFC position, with MFC 8 producing the lowest power of 47 μW. For all MFCs, the polarisation curves showed that power was mainly limited by mass transfer losses, visible in the high current region, whereas nearly no activation losses (visible in the low current region) were observed (Larminie & Dicks 2003). By reducing the amount of C/E in the anolyte, the mass transfer losses occurred sooner, ultimately limiting the power generation. The power curves for AUM 2× in Figure 2(a)–(d) indicate an 'overshoot' trend for all MFCs, which tends to rise to a higher power, but then rapidly decreases in both current and voltage terms (Winfield *et al.* 2011a). In MFC 5 for AUM 5× (Figure 2(c)) the maximum power points (MPP) were not directly limited by this type of loss, however this was the case for the MFCs further downstream; MFC 6, 7 (data not shown), and MFC 8 (Figure 2(d)).

The sequential downstream decrease in power was more marked when the fuel cells were fed AUM 15×. Decreasing MPPs in the numerical order of the cascade can be explained by the reduction of available nutrients by the preceding MFC, thus resulting in more dilute influents reaching the downstream MFCs. With AUM 2× and 5×, significantly lower MPPs were obtained (ca. 20–40 μW) with mass transfer losses limiting the performance, especially for the downstream MFCs. The findings for different nutrient concentrations are in agreement with previous studies on small-scale MFC cascades (Winfield *et al.* 2012). The decrease in power performance could be explained by the behaviour of the internal resistance (R_{INT}) of all eight MFCs for the three substrates, since the R_{INT} of each MFC was reduced with increasing concentrations of nutrients. This was likely due to the increase in conductivity of the anolyte, measured to be: tap water/800; AUM 2×/24,048; AUM 5×/25,216 and AUM 15×/26,440 μS/cm.

Effects of high nutrient concentration (AUM 15×) over time

To determine the effect of increasing the available nutrients on the development of the anodic biofilm, the cascade was

fed for 6 days with AUM 15× with polarisation experiments performed on days 2, 4 and 6. Figure 3 shows the development of the MPPs (a) and the R_{INT} (b) for the period of 6 days.

The MPP increased with time for all MFCs (see Figure 3(a)), however the rate of increase for MFCs 6–8 is lower than that of MFCs 1–5. This is reflected in the higher increases in R_{INT} for MFCs 6–8 (Figure 3(b)), compared to very small increases during the first 4 days, and almost no increase between days 4 and 6 for MFCs 1–5, which is consistent with Winfield *et al.* (2012). The constant behaviour of the MFCs 1–5 R_{INT} was due to the more enriched and more conductive influent reaching those units first.

Maximum power output

The highest power recorded was 116.96 μW, (power density 116.96 W/m^3 – total anode chamber volume; 77.97 mW/m^2 – total anode surface area; 974.66 mW/m^2 – projected a surface area), by MFC1 fed with AUM 15× for 6 days (Figure 4). As can be seen, the strongest MFC1 also showed negligible mass transfer losses and the lowest R_{INT} compared to all the other MFCs in the cascade.

The power output produced by MFC1 is higher than that reported for MFCs with comparable anode chamber volumes, however the experimental conditions were significantly different, in terms of the anode electrode surface area, cathodic half-cell and anolyte flow rate (Ieropoulos

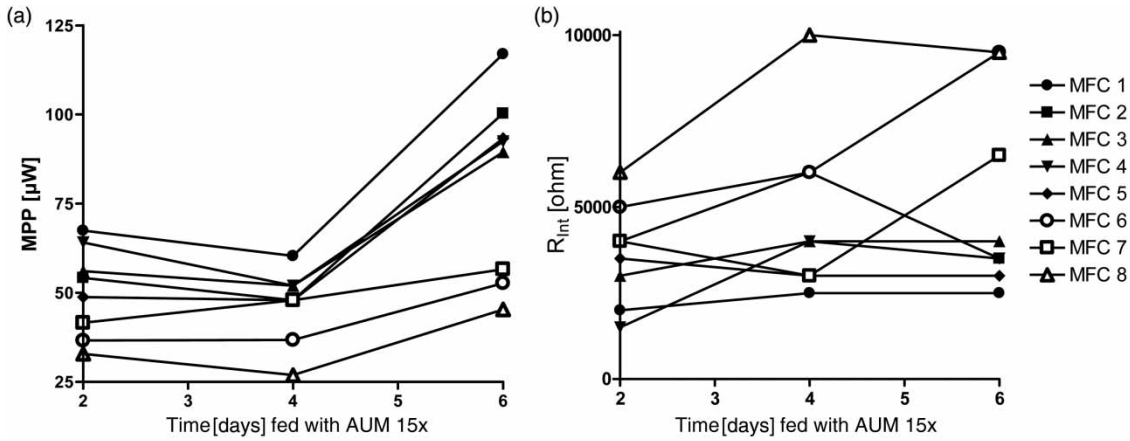

Figure 3 | MPP (a) and R_{INT} (b) of each MFC in the cascade over 6 days fed with AUM 15×.

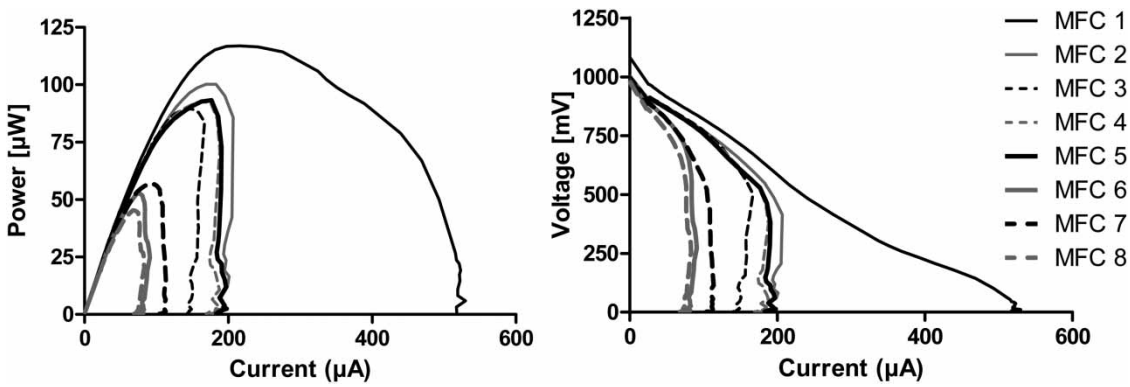

Figure 4 | Power (left) and polarisiton curves (right) 6 days after the anolyte of the cascade was changed to AUM 15×.

et al. 2010d; Winfield et al. 2012). It can therefore be assumed that the low exchange volume of the MFCs in the current study, mainly due to a lower hydraulic retention time (HRT; ca. 12.69 minutes), might have assisted in overcoming the diffusion limitations due to the advective flow in MFC1. The high MPP might also be an indicator for conditions of electron spilling by the anodophilic organisms (Russell 2007).

Stability in power output

To confirm that each stage of the cascade can produce a constant power over time, the output of all eight MFCs were monitored with two different loads (10 and 3.3 kΩ) over a period of 39 h after initial stabilisation. Figure 5 shows that the order of the produced voltages for each MFC corresponds to their position in the cascade (except MFC6), and more divergence between performances was recorded for the lower load (3.3 kΩ).

The average power produced per MFC was 40.86 and 50.26 μW under 10 and 3.3 kΩ loads, respectively. Under the 10 kΩ load the difference between the weakest and strongest MFCs was only 51.2% (MFC8 28.27 μW; MFC1 55.07 μW), whereas under the 3.3 kΩ load, the weakest MFC8 produced a mere 13.6% (15.36 μW) of the power generated by MFC 1 (113.18 μW).

These results therefore suggest that a decreasing performance in downstream MFCs is more pronounced as heavier loads are applied. This indicates a relationship between metabolic rate and applied load, since increased metabolism in upstream MFCs results in a decreased nutrient supply in downstream MFCs (Ledezma et al. 2013). Relationships like this can be exploited in stack design and development for dynamic *in-situ* adjusting and reconfiguration (Winfield et al. 2011b).

Electrical stack

Polarisation experiments were performed for the different stack connections in order to determine the best configuration for operating practical applications. The polarisation and power curves are shown in Figure 6: (a) 'series'; (b) 'parallel'; (c) '2(4)-series' and (d) '4(2)-series'. Figure 6(a) shows that the open circuit voltage of all MFCs connected in series was 3.1 V, which is approximately one-third of the expected 9 V (sum of all individual MFC voltages – data not shown) and, as can be seen, the ohmic losses were the main performance limitation. The lower than the theoretical maximum open circuit voltage and the severe ohmic losses under the series condition can be explained by the 'short-circuit' effect of the fluidic links between the MFCs in the cascade, which provide an alternative path for electrons to flow. Fluidic isolation between MFCs has been previously reported as a critical factor in stacks (Ieropoulos et al. 2008, 2010a), however the objective of sequential artificial urine treatment in the current study could only be achieved through fluidic linkage between MFCs. The all-in series configuration was nevertheless a valuable test to reveal the degree of losses from such a sub-optimal (in electrical terms) arrangement.

The open circuit voltage of the stack in 'parallel' was 1.1 V, which is the mean of the individual MFCs open circuit voltage. This configuration produced a maximum current of 1.227 mA and the highest MPP (271 μW at

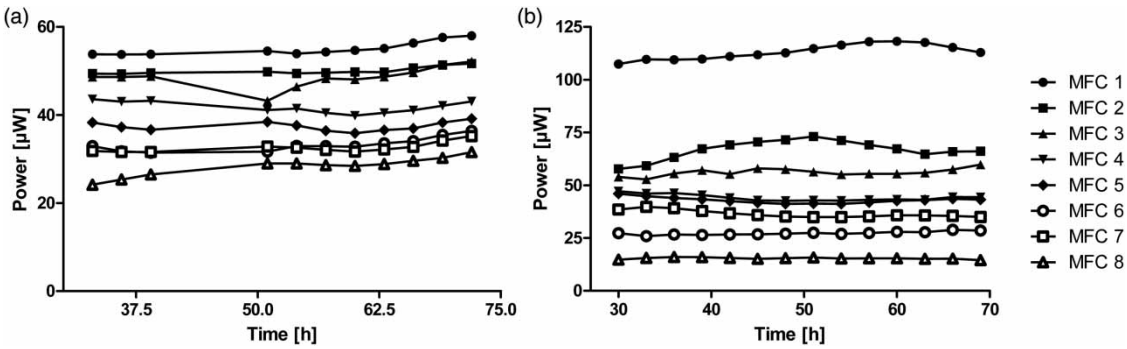

Figure 5 | Power measured over 39 h with 10 kΩ (a) and 3.3 kΩ (b) loads, following output stabilisation (substrate AUM 15×).

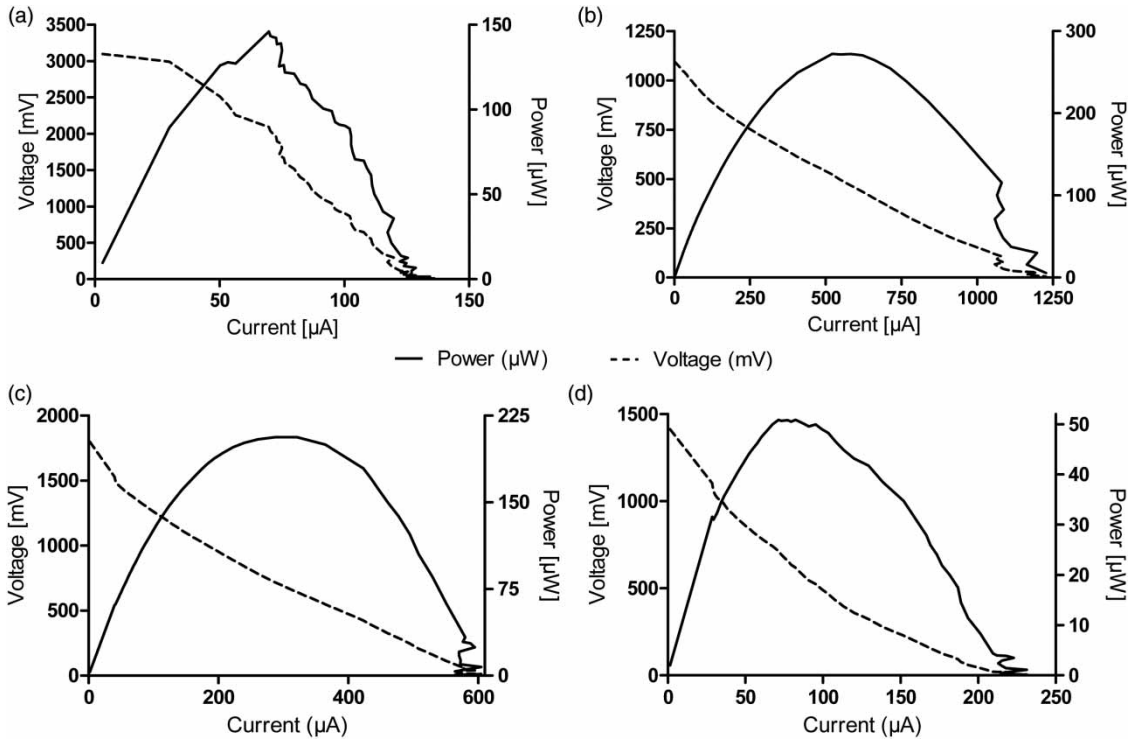

Figure 6 | Power and polarisation curves for the stack configurations: (a) series; (b) parallel; (c) '2(4)-series'; (d) '4(2)-series'.

574 μA), but the lowest operating voltage at the MPP (495 mV).

Practical implementation: LED and dc-motor powered windmill

To show the feasibility of MFCs powering real applications, the 'series' configuration was used to operate a red LED, which performed successfully at a constant voltage of 1.63 V, with a 40 μA current consumption (video documentation available upon request). The more energy demanding small wooden windmill required the MFCs to be configured in the '2(4)-series', which charged the 5 Farad capacitor from 20 to 780.90 mV over 280 minutes. The produced current dictated the rate of charge (Duncan 1997). The windmill was operated from the charged capacitors for 217 seconds and the motor stopped moving at 171 mV (video documentation available upon request).

The results in Figure 6 show that it was necessary to use a combined series/parallel configuration (Ieropoulos *et al.* 2010a; Winfield *et al.* 2012) of two groups of 4-in-parallel MFCs, connected in series (Figure 6(c)). This showed the best level of working voltage (642 mV), current (312 μA) and power (206 μW).

CONCLUSIONS

The experiments presented in this paper have demonstrated the utilisation of artificial urine in novel 2 mL small-scale MFCs for power generation. By increasing the amounts of carbon/energy concentration in the AUM, the power generation of all MFCs increased, in relation to their position in the cascade. The energy generated by the small-scale stack fuelled by artificial urine was used to power two different demonstrators; an LED and a dc-motor-driven windmill. This is a significant breakthrough and an important step into the future, where collectives of MFCs can actually be used to operate real applications. In this particular study a total of 8 mL (anode volume) was sufficient to charge a 5 F capacitor, resulting in an energy transfer of 1.5 J. Power output and wastewater treatment efficiency are

inherently linked in MFCs, since the power output is in direct proportion to chemical oxygen demand (COD) breakdown and reduction. Therefore the more powerful a MFC system is, the more valuable it would become for sanitation improvement. For the sake of comparison, EcoBot-III was powered by 48×6.25 mL MFCs (300 mL total anode chamber volume), each producing approximately 50 μW and charging a 0.8 F capacitor bank (Ieropoulos *et al.* 2010b). Calculated on the average MPP of the MFCs in the cascade reported herewith, a theoretical projection suggests that only 30 of these 2 mL small-scale MFCs (total volume 60 mL) would be sufficient to operate EcoBot-III now. This emphasises the benefits of continuous flow miniaturised MFCs for maximising energy production from an abundant fuel source such as urine.

FUTURE DIRECTIONS

The work described here is part of a larger study funded by the Bill and Melinda Gates Foundation and the UK EPSRC that is also investigating the potential for the technology to kill pathogens and also produce clean water. If in addition to generating electricity as a result of cleaning up an abundant waste product both these milestones can be achieved, then the future use of MFCs to globally benefit humankind is becoming a reality.

ACKNOWLEDGEMENTS

This work is funded by the Bill and Melinda Gates Foundation grant no. OPP1044458 and the UK Engineering and Physical Sciences Research Council, grant no EP/I004653/1.

REFERENCES

Brooks, T. & Keevil, C. W. 1997 A simple artificial urine for the growth of urinary pathogens. *Lett. Appl. Microbiol.* **24** (3), 203–206.

Degrenne, N., Buret, F., Allard, B. & Bevilacqua, P. 2012 Electrical energy generation from a large number of microbial fuel cells operating at maximum power point electrical load. *J. Power Sources* **205**, 188–193.

Duncan, T. (ed.) 1997 *Quantification of the Internal Resistance Distribution of Microbial Fuel Cells*, 2nd edn. John Murray Ltd., London.

Fangzhou, D., Zhenglong, L., Shaoqiang, Y., Beizhen, X. & Hong, L. 2011 Electricity generation directly using human feces wastewater for life support system. *Acta Astronaut.* **68** (9–10), 1537–1547.

Futamata, H., Bretschger, O., Cheung, A., Kan, J., Owen, R. & Nealson, K. H. 2012 Adaptation of soil microbes during establishment of microbial fuel cell consortium fed with lactate. *J. Biosci. Bioeng.* **115** (1), 58–63.

Harnisch, F. & Schröder, U. 2010 From MFC to MXC: chemical and biological cathodes and their potential for microbial bioelectrochemical systems. *Chem. Soc. Rev.* **39** (11), 4433–4448.

He, Z., Liu, J., Qiao, Y., Li, C. M. & Tan, T. T. Y. 2012 Architecture engineering of hierarchically porous chitosan/vacuum-stripped graphene scaffold as bioanode for high performance microbial fuel cell. *Nano Lett.* **12** (9), 4738–4741.

Ieropoulos, I. 2006 EcoBot: Towards an Energetically Autonomous Robot. PhD Thesis. University of the West of England, Bristol, UK.

Ieropoulos, I., Greenman, J. & Melhuish, C. 2008 Microbial fuel cells based on carbon veil electrodes: stack configuration and scalability. *Int. J. Energy Res.* **32**, 1228–1240.

Ieropoulos, I., Greenman, J. & Melhuish, C. 2010a Improved energy output levels from small-scale Microbial Fuel Cells. *Bioelectrochemistry* **78** (1), 44–50.

Ieropoulos, I., Greenman, J. & Melhuish, C. 2010b EcoBot-III: a robot with guts. In: *Proceedings of the Alife XII conference. 2010*, Denmark, pp. 733–740.

Ieropoulos, I., Winfield, J. & Greenman, J. 2010c Effects of flow-rate, inoculum and time on the internal resistance of microbial fuel cells. *Bioresour. Technol.* **101**, 1190–1198.

Ieropoulos, I., Greenman, J. & Melhuish, C. 2010d Small scale microbial fuel cells and different ways of reporting output. *ECS Trans.* **28** (9), 1–9.

Ieropoulos, I., Greenman, J. & Melhuish, C. 2012 Urine utilisation by microbial fuel cells; energy fuel for the future. *Phys. Chem. Chem. Phys.* **14** (1), 94–98.

Larminie, J. & Dicks, A. 2003 *Fuel Cell Systems Explained*. Wiley, Chichester, UK.

Ledezma, P., Greenman, J. & Ieropoulos, I. 2012 Maximising electricity production by controlling the biofilm specific growth rate in microbial fuel cells. *Bioresour. Technol.* **32**, 1228–1240.

Ledezma, P., Stinchcombe, A., Greenman, J. & Ieropoulos, I. 2013 The first self-sustainable microbial fuel cell stack. *Phys. Chem. Chem. Phys.* **15** (7), 2278–2281.

Liu, X., Du, X., Wang, X., Li, N., Xu, P. & Ding, Y. 2012 Improved microbial fuel cell performance by encapsulating microbial cells with a nickel-coated sponge. *Biosens. Bioelectron.* **41**, 848–851.

Qian, F. & Morse, D. E. 2011 Miniaturizing microbial fuel cells. *Trends Biotechnol.* **29** (2), 62–69.

Russell, J. B. 2007 The energy spilling reactions of bacteria and other organisms. *J. Mol. Microb. Biotechnol.* **13** (1–3), 1–11.

Winfield, J., Ieropoulos, I. & Greenman, J. 2012 Investigating a cascade of seven hydraulically connected microbial fuel cells. *Bioresour. Technol.* **110**, 245–250.

Winfield, J., Ieropoulos, I. A., Greenman, J. & Dennis, J. 2011a The overshoot phenomenon as a function of internal resistance in microbial fuel cells. *Bioelectrochemistry* **81**, 22–27.

Winfield, J., Ieropoulos, I. A., Greenman, J. & Dennis, J. 2011b Investigating the effects of fluidic connection between microbial fuel cells. *Bioprocess Biosyst. Eng.* **34**, 477–484.

Yu, J., Park, Y., Cho, H., Chun, J., Seon, J., Cho, S. & Lee, T. 2012 Variations of electron flux and microbial community in air-cathode microbial fuel cells fed with different substrates. *Water Sci. Technol.* **66** (4), 748–753.

Zhang, G., Wang, K., Zhao, Q., Jiao, Y. & Lee, D.-J. 2012 Effect of cathode types on long-term performance and anode bacterial communities in microbial fuel cells. *Bioresour. Technol.* **118**, 249–256.

First received 25 September 2012; accepted in revised form 13 February 2013. Available online 27 April 2013